Multi-Objective Planning for Reactive Power Compensation of Radial Distribution Networks With Unified Power Quality Conditioner Allocation Using Particle Swarm Optimization

Sanjib Ganguly, *Member, IEEE*

***Abstract*—This paper presents a particle swarm optimization (PSO)-based multi-objective planning algorithm for reactive power compensation of radial distribution networks with unified power quality conditioner (UPQC) allocation. A UPQC consists of a series and a shunt inverter. The UPQC model based on phase angle control (UPQC-PAC) is used. In UPQC-PAC, the series inverter injects a voltage with controllable phase angle in such a way that the voltage magnitude at load end remains unchanged. Due to the phase angle shift, the series inverter participates in load reactive power compensation along with the shunt inverter during healthy operating condition. In the proposed approach, the optimal location, the optimal reactive power compensation required at the location, and the optimal design parameters of UPQC are determined by minimizing three objective functions: 1) the rating of UPQC, 2) network power loss, and 3) percentage of nodes with undervoltage problem. These objectives are simultaneously minimized to obtain a set of non-dominated solutions using multi-objective PSO (MOPSO). The performances of two MOPSO variants are compared and the better one is used in all subsequent studies. A load flow algorithm including the UPQC-PAC model is devised. The performance of the proposed algorithm is validated with different case studies.**

***Index Terms*—Multi-objective optimization, power distribution planning, reactive power, unified power quality conditioner.**

I. Introduction

An optimal reactive power compensation can significantly improve the performance of a radial distribution network by reducing its power loss and improving its voltage profile, and line loadability. There are several reactive power compensation strategies reported time-to-time in the literature, for example capacitor placement [1], [2], combined operation of on-load tap changer and capacitor banks [3], and integration of distributed generation (DG) [4], [5]. The latest addition is the distribution FACTS (DFACTS) device allocation. Although DFACTS devices are traditionally used in power quality improvement they can be used in optimal reactive power compensation as well. In [6], the optimal allocation of distribution static compensator (DSTATCOM) is carried out to minimize network power loss and to improve node voltage magnitude. The unified power quality conditioner (UPQC) is one of the versatile DFACTS devices [7]. The research on UPQC is mostly focused on the mitigation of power quality problems for single load [7]–[10]. The theme of this paper is set as an investigation of its potential applicability in optimal reactive power compensation of a distribution network.

A UPQC consists of a shunt and a series inverter [7]. The shunt inverter provides reactive power and harmonic compensations by injecting a shunt current to the load. The series inverter is used in the mitigation of voltage related problems, for example sag and swell in supply voltage by injecting a controllable series voltage. These two inverters are connected back-to-back with a DC link and this becomes the most common form of UPQC structure after its practical implementation reported in [8]. There are various UPQC models, such as UPQC-P, UPQC-Q, UPQC-S, and UPQC-$\mathrm{VA}_{\min}$. The series inverter only provides active power in UPQC-P and reactive power in UPQC-Q by injecting a controllable in-phase and a controllable quadrature voltage, respectively so as to mitigate voltage sag problem. A comparative performance assessment of these two models is given in [9]. The series inverter in UPQC-S can simultaneously provide both real and reactive powers [10]. In UPQC-$\mathrm{VA}_{\min}$ [11], the optimum angle of the injected voltage of the series inverter is determined to minimize the VA rating of UPQC. Mostly, the research on UPQC is focused on the following attributes:

- development of different series compensation schemes, for example UPQC-P, UPQC-Q, and UPQC-S [9]–[11];
- development of new UPQC topology/structure, for example, 3-phase 4 wire structure [12], interline UPQC [13] in which these two inverters are placed in different feeders of a network, and UPQC without the common DC link, i.e., OPEN UPQC [14];
- development of new control strategy for UPQC, for example phase angle control [15], simultaneous voltage and current compensation scheme [16], and particle swarm optimization based feedback controller [17];
- minimization of the cost/VA rating of UPQC [11], [18];
- combined operation with DG [19], [20].

In almost all works, a UPQC is designed to protect a single load which is assumed to be the most sensitive load. But, a network may consist of multiple equally sensitive loads. In that case, an optimal location for UPQC in a network is of an interest. In general, the sag/swell in supply voltage is short du-

Manuscript received July 08, 2013; revised November 14, 2013; accepted December 22, 2013. Date of publication January 15, 2014; date of current version June 16, 2014. Paper no. TPWRS-00878-2013.

The author is with the Department of Electrical Engineering, National Institute of Technology, Rourkela, India (e-mail: sanjib191@gmail.com).

Digital Object Identifier 10.1109/TPWRS.2013.2296938

ration phenomena. Thus, to get the maximum utilization of a UPQC, its potential use in reactive power compensation during healthy operating conditions should be investigated. But, less attention is put on this aspect in the literature. In [21], a work on UPQC allocation for under voltage mitigation of distribution networks is reported. But, constant shunt compensation is used irrespective of the load demand and location of a UPQC in a network. Hence, it is not a realistic approach.

A modified design of the phase angle control model for UPQC (UPQC-PAC) [15] is proposed in this work. In the UPQC-PAC, the series inverter injects a controllable series voltage so as to shift the phase angle of the load voltage. Due to this phase shift, the series inverter participates in load-reactive power compensation along with the shunt inverter and helps in reduction of the VA rating of the shunt inverter. In [15], UPQC is modeled for the reactive power compensation of a single load. Thus, its design is slightly modified so that a UPQC can be capable of providing the reactive power compensation of a distribution network. In addition, the total harmonic distortion (THD) of the load current is included in the model and used in the determination of VA rating of the shunt inverter. A distribution system load flow algorithm including the UPQC-PAC model is devised and used as a support subroutine of the planning algorithm.

To determine the optimal location and parameters of UPQC, a multi-objective planning model is formulated with three objective functions. They are minimization of: 1) the rating of the UPQC, 2) network power loss, and 3) percentage of nodes with undervoltage problem (PNUVP). The simultaneous optimization of these objectives is carried out using Pareto-dominance principle [22] to obtain a set of non-dominated solutions called Pareto-approximation set, in which no solution is inferior to other. The solution strategy used is particle swarm optimization (PSO) [23] for its easy implementation, effective memory use, and an efficient maintenance of the solution diversity. Its performance is also tested on a number of power system problems [24]. Since PSO is a multi-point search algorithm, it can provide a set of non-dominated solutions in a single run. There are many Pareto-based multi-objective PSO (MOPSO) variants [25]. In this work, two MOPSO variants are chosen. They are: non-dominated sorting MOPSO (NSMOPSO) [26] and strength Pareto evolutionary algorithm-2 [27] (SPEA2)-based MOPSO (SPEA2-MOPSO) [28]. Their performances on the present problem are compared and the better one is used in subsequent studies. The planning approach is validated on a 33-node and a 69-node distribution networks. Different case studies are carried out and the results are analyzed. The results obtained with the proposed algorithm are found to be better as compared to the approaches reported in [6] and [21].

The paper is organized as follows: In Section II, the UPQC-PAC model and its inclusion strategy in radial distribution network load flow are described. The multi-objective reactive power compensation planning model with UPQC allocation is formulated in Section III. The multi-objective reactive power compensation planning algorithm using MOPSO is provided in Section IV. The simulation study is presented in Section V. Section VI concludes the paper.

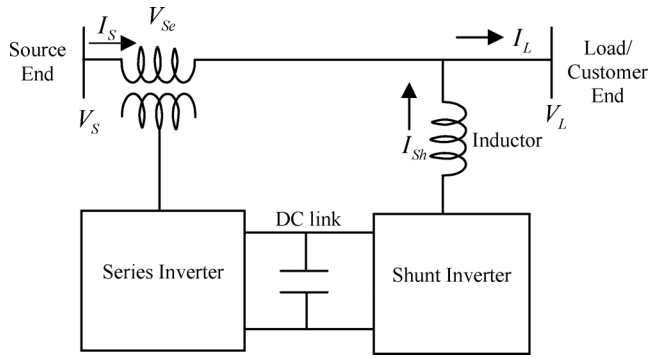

Fig. 1. Basic schematic of UPQC.

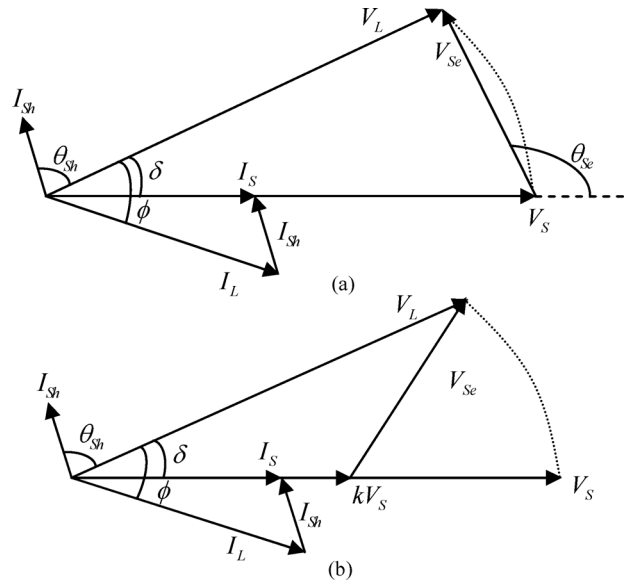

Fig. 2. Phasor diagram of shunt and series compensations of UPQC-PAC operating: (a) at normal/healthy condition and (b) at voltage sag.

II. UPQC-PAC Model for Distribution Networks

The basic schematic of a UPQC is shown in Fig. 1. In general, the series inverter is used in mitigation of sag and swell of supply voltage and the shunt inverter is used in compensations of the reactive component of load current and harmonics [7]. The series inverter injects a series voltage (V_{Se}) and the shunt inverter injects a shunt compensating current (I_{Sh}) during healthy condition as well as during voltage sag, as shown in Fig. 2(a) and (b), respectively. In the UPQC-PAC model, the series inverter injects V_{Se} during healthy operating condition to create a phase angle (δ) shift of the load end voltage. This helps the series inverter in providing the reactive power and thereby it reduces the rating for the shunt inverter and the overall rating of a UPQC to some extent [15]. During voltage sag, the load end voltage is kept constant by injecting V_{Se}. The magnitude of V_{Se} depends on the maximum rating of the series inverter. The VA ratings of both the inverters are determined according to Fig. 2(a).

A. Determination of VA Rating for the Series Inverter

The VA-rating of the series inverter depends on the injected voltage (V_{Se}) and the compensated source end current (I_S) as given in the following:

$$S_{Se} = V_{Se} I_S. \tag{1}$$

During healthy condition, the series voltage is computed as

$$V_{Se} = \sqrt{V_L^2 + {V_S}^2 - 2V_L V_S \cos\delta}. \tag{2}$$

The voltage magnitude at the source and load ends are kept same, i.e., $[V_L = V_S]$. So

$$\begin{aligned} V_{Se} &= \sqrt{V_S^2 + {V_S}^2 - 2V_S V_S \cos\delta} \\ &= V_S\sqrt{2(1-\cos\delta)}. \end{aligned} \tag{3}$$

Assuming a UPQC to be lossless, the active power demanded by the load is equal to the active power drawn from the source [29]. Hence

$$V_S I_S = V_L I_L \cos\phi \tag{4}$$

$$I_S = I_L \cos\phi. \tag{5}$$

From (1), (3), and (5), the VA-rating of the series inverter is determined as

$$S_{Se} = V_S I_L \cos\phi\sqrt{2(1-\cos\delta)}. \tag{6}$$

B. Determination of VA Rating for the Shunt Inverter

The VA rating of the shunt inverter depends on the load end voltage (V_L) which is equal to the source voltage (V_S) and the compensating current (I_{Sh}) provided by the shunt inverter as given in the following:

$$S_{Sh} = V_S I_{Sh}. \tag{7}$$

According to Fig. 2, the compensating current can be determined as

$$I_{Sh} = \sqrt{I_S^2 + I_L^2 - 2I_S I_L \cos(\phi-\delta)}. \tag{8}$$

From (5) and (8)

$$I_{Sh} = I_L\sqrt{1+\cos^2\phi - 2\cos\phi\cos(\phi-\delta)}. \tag{9}$$

As noted above, one of the basic functions of UPQC is harmonic compensation. Thus, the THD of load current is included in the model. THD is defined as the ratio of the distortion component of the current (I^{dis}) to the fundamental component (I^f):

$$THD = \frac{I^{dis}}{I^f}. \tag{10}$$

The shunt inverter of UPQC provides a compensating current (I_{Sh}^{dis}) so as to neutralize the distortion component of the load current (I_L^{dis}) [11], i.e.,

$$I_L^{dis} = I_{Sh}^{dis}. \tag{11}$$

From (10) and (11)

$$THD_L I_L^f = THD_{Sh} I_{Sh}^f \tag{12}$$

where THD_L and THD_{Sh} are THD of load current and shunt compensating current, respectively. From (9) and (12)

$$THD_{Sh} = \frac{THD_L}{\sqrt{1+\cos^2\phi - 2\cos\phi\cos(\phi-\delta)}}. \tag{13}$$

The r.m.s value of shunt compensating current is obtained as

$$I_{Sh} = I_{Sh}^f\sqrt{1+THD_{Sh}^2}. \tag{14}$$

From (9), (13), and (14), the shunt compensating current is determined as

$$I_{Sh} = I_L^f\sqrt{1+\cos^2\phi - 2\cos\phi\cos(\phi-\delta) + THD_L^2}. \tag{15}$$

From (7) and (15), the expression for the VA rating of the shunt inverter is found as

$$S_{Sh} = V_S I_L^f\sqrt{1+\cos^2\phi - 2\cos\phi\cos(\phi-\delta) + THD_L^2}. \tag{16}$$

C. Active and Reactive Power Provided by the Inverters

The active (P_{Se}) and reactive power (Q_{Se}) delivered by the series inverter can be determined as

$$P_{Se} = S_{Se}\cos\theta_{Se} \tag{17}$$

$$Q_{Se} = S_{Se}\sin\theta_{Se}. \tag{18}$$

Similarly, the active (P_{Sh}) and reactive power (Q_{Sh}) delivered by the shunt inverter are

$$P_{Sh} = S_{Sh}\cos\theta_{Sh} \tag{19}$$

$$Q_{Sh} = S_{Sh}\sin\theta_{Sh}. \tag{20}$$

The angle θ_{Se} and θ_{Sh} are determined as [15]

$$\theta_{Se} = 180^0 - \tan^{-1}\left\{\frac{\sin\delta}{(1-\cos\delta)}\right\} = 90^0 + \frac{\delta}{2}. \tag{21}$$

There are two possibilities that: 1) $\delta > \phi$ and 2) $\delta < \phi$. For the first case, the expression for the angle θ_{Sh} is found to be

$$\theta_{Sh} = \tan^{-1}\left[\frac{\{\cos(\delta-\phi) - \cos\phi\}}{\sin(\delta-\phi)}\right] + 90^0 - \delta. \tag{22}$$

For the second case, the expression for the angle θ_{Sh} is obtained as

$$\theta_{Sh} = \tan^{-1}\left[\frac{\{\cos(\phi-\delta) - \cos\phi\}}{\sin(\phi-\delta)}\right] + 90^0 - \delta. \tag{23}$$

The total reactive power delivered by a UPQC is

$$Q_{UPQC} = Q_{Se} + Q_{Sh}. \tag{24}$$

D. Determination of Phase Angle δ

The maximum value of the series injected voltage ($V_{Se_{\max}}$) is assumed to be a certain fraction of the desired load voltage, i.e., $V_{Se_{\max}} = K_{Se}V_L$ (K_{Se} = ratio of the maximum series injected voltage to the desired load voltage). It is determined by using (3):

$$V_{Se_{\max}} = V_S\sqrt{2(1-\cos\delta_{\max})} = K_{Se}V_L. \tag{25}$$

Since the relationship $V_L = V_S$ is maintained, the maximum phase angle is obtained as

$$\delta_{\max} = \cos^{-1}(1 - 0.5K_{Se}^2). \tag{26}$$

From (18), (21), and (25), the maximum reactive power that the series inverter can provide (i.e., $Q_{Se^i_{\max}}$) is determined:

$$\begin{aligned} Q_{Se^i_{\max}} &= V_S I_S\sqrt{2(1-\cos\delta_{\max})}\sin(90^0 + 0.5\delta_{\max}) \\ &= V_S I_S \sin\delta_{\max}. \end{aligned} \tag{27}$$

If the reactive power compensation required at a node, at which a UPQC is placed (say node i) is $Q_{Comp}(i)$, the maximum reactive power that the shunt inverter has to provide is

$$Q_{Sh^i_{\max}} = Q_{Comp}(i) - Q_{Se^i_{\max}}. \tag{28}$$

If $Q_{Sh^i_{\max}}$ is found to be higher than the maximum reactive power compensation capacity of a shunt inverter, i.e., S_{Sh}, it is set at its maximum value. For reactive power demand at node i [i.e., $Q_L(i)$], the reactive power required from the series inverter becomes

$$Q_{Se^i} = Q_L(i) - Q_{Sh^i_{\max}}. \tag{29}$$

From (6), (18), and (21)

$$\begin{aligned} Q_{Se^i} &= V_S(i)I_L(i)\cos\phi_i\sqrt{2(1-\cos\delta_i)}\sin\left(90^0 + \frac{\delta_i}{2}\right) \\ &= V_S(i)I_S(i)\sin\delta_i. \end{aligned} \tag{30}$$

From (30), the phase angle for the series injected voltage at node i (δ_i) is computed as

$$\delta_i = \sin^{-1}\left[\frac{Q_{Se^i}}{\{V_S(i)I_S(i)\}}\right]. \tag{31}$$

E. UPQC-PAC in Voltage Sag Mitigation

A UPQC-PAC can also be used in voltage sag mitigation by injecting the series voltage according to Fig. 2(b). Suppose, the source end voltage (V_S) is reduced to kV_S ($0 \le k < 1$) due to k_{Sag} p.u. sag in source voltage (where, $k_{Sag} = 1 - k$). The amount of voltage sag that can possibly be mitigated using the maximum series injected voltage ($V_{Se_{\max}} = K_{Se}V_L$), used in reactive power compensation, can be determined as

$$V_L^2 + (kV_S)^2 - 2V_L(kV_S)\cos\delta = V_{Se_{\max}}^2. \tag{32}$$

Putting $V_{Se_{\max}} = K_{Se}V_L$ and $V_S = V_L$ in (32),

$$k^2 - 2k\cos\delta + 1 - K_{Se}^2 = 0. \tag{33}$$

The solutions of (33) are:

$$k = \cos\delta \pm \sqrt{\cos^2\delta + K_{Se}^2 - 1} \tag{34}$$

Therefore the value of k_{Sag} can be obtained as

$$k_{Sag} = 1 - k = 1 - \left(\cos\delta \pm \sqrt{\cos^2\delta + K_{Se}^2 - 1}\right). \tag{35}$$

From (26) and (35), a unique feasible solution for maximum value of k_{Sag} is obtained as

$$k_{Sag_{\max}} = K_{Se}^2. \tag{36}$$

It is observed that higher value of K_{Se} is required to mitigate higher amount of voltage sag. But, this increases the VA rating of the UPQC. Hence, the choice of K_{Se} requires a compromise between the rating of UPQC and the desirable amount of sag mitigation.

F. Distribution System Load Flow With UPQC-PAC Model

To study the impact of the UPQC allocation in distribution networks, the UPQC-PAC model is incorporated in the forward-backward sweep load flow algorithm [30], which consists of two steps:

- *Backward sweep*: In this step, the load current of each node of a distribution network having N number of nodes is determined as

$$\overline{I}_L(m) = \left\{\frac{P_L(m) - jQ_L(m)}{\overline{V}^*(m)}\right\} \quad [\mathrm{m} = 1, \ldots, N] \tag{37}$$

  where $P_L(m)$ and $Q_L(m)$ represent the active and reactive power demand at node m and the overbar notation (-) indicates the phasor quantities, such as $\overline{I}_L$, $\overline{V}$. Then, the current in each branch of the network is computed as

$$\overline{I}(mn) = \overline{I}_L(n) + \sum_{m\in\Gamma}\overline{I}_L(m) \tag{38}$$

  where the set Γ consists of all nodes which are located beyond the node n [30]. To incorporate the shunt inverter model, the reactive power demand at the node at which the UPQC is placed, say, at node i, is modified by

$$Q_L{}'(i) = Q_L(i) - Q_{Sh^i_{\max}}. \tag{39}$$

- *Forward sweep*: This step is used after the backward sweep so as to determine the voltage at each node of a distribution network as follows:

$$\overline{V}(n) = \overline{V}(m) - \overline{I}(mn)Z(mn) \tag{40}$$

where nodes n and m represent the receiving and sending end nodes, respectively for the branch mn and $Z(mn)$ is the impedance of the branch. The series inverter model is incorporated by advancing the phase angle of the voltage of the node at which the UPQC is placed (i.e., node i) by the phase shift angle δ_i as given in the following:

$$\overline{V}(i) = V_{DL}\angle(\alpha_i + \delta_i) \tag{41}$$

where α_i is the phase angle of the voltage at node i before UPQC placement and V_{DL} is the desired load voltage.

III. Multi-Objective Planning Model for Reactive Power Compensation With UPQC Allocations

In the proposed planning approach, a multi-objective planning model is formulated to determine the optimal location for UPQC, the optimal amount of reactive power compensation required at the location, and the optimal value of K_{Se}. These optimizing variables are determined by minimizing three objective functions. They are: 1) VA rating of the UPQC, 2) network power loss, and 3) percentage of nodes with undervoltage problem (PNUVP) compared to the uncompensated network (i.e., without UPQC). The *objective function* 1 deals with system economy and its minimization provides an economical solution. The *objective functions* 2 and 3 are the performance measures of a network. The minimization of these objectives is required to obtain better performance a network. The expressions for these objective functions are given as follows:

$$Objective\ function\ 1 : S_{UPQC} = S_{Sh} + S_{Se} \tag{42}$$

$$Objective\ function\ 2 : P_{Loss}^{UPQC} = \sum_{jk\in\Upsilon} \{I_L(mn)\}^2 r(mn) \tag{43}$$

$$Objective\ function\ 3 : PNUVP = 100\left(\frac{N_{UPQC}^{UV}}{N_{Base}^{UV}}\right) \tag{44}$$

where $I_L(mn)$ and $r(mn)$ represent line current and resistance of the branch mn. The set Υ consists of all branches in a network. N_{UPQC}^{UV} and N_{Base}^{UV} represent number of nodes with under voltage problem with and without UPQC allocations, respectively. Basically, the denominator of the objective function 3 is used to understand the degree of undervoltage mitigation taking place due to the UPQC allocation.

The optimization is carried out under the following constraints:

1) A UPQC is designed so that it can mitigate a given maximum value of voltage sag, if required. Thus, the value of K_{Se} is to be kept above the minimum value required to mitigate the given maximum amount of voltage sag. It can be derived by using (36).
2) The total reactive power delivered by a UPQC is to be kept below the sum of the reactive power demand of all nodes in a network, i.e., $0 < Q_{UPQC} \leq \left\{\sum_{j=1}^{N} Q_L(j)\right\}$.
3) The line current (I_{ij}) is to be kept below the thermal limit of the line, i.e., $I_{ij} \leq I_{ij}^{Th}$ ($I_{ij}^{Th} =$ thermal limit of line ij).

Each node except the substation node is considered as a candidate node for the UPQC allocation.

The objective function 1 conflicts with the objective functions 2 and 3, since the minimization of the network power loss and the PNUVP require higher rating for the UPQC. This requires multi-objective optimization approach to obtain a set of non-dominated solutions, in which none is superior to other [22]. Each solution provides a different combination of location and rating for UPQC. Finally, a solution can be selected from the set according to the requirement and investment budget of a utility. For example, if a utility desires to implement the solution corresponding to the lowest power loss its investment becomes the highest because the MVA rating for the solution is highest. There are different multi-objective optimization approaches [22], for example weighted aggregation, Pareto-based approach, lexicographic ordering etc. In this work, the Pareto-based approach is used. The optimization is performed considering three cases:

- *Case A*: Simultaneous optimization of the objective functions 1 and 2
- *Case B*: Simultaneous optimization of the objective functions 1 and 3
- *Case C*: Simultaneous optimization of the objective functions 1, 2, and 3

A. Pareto-Dominance Principle

The Pareto-dominance principle [22] states that, for an M-objective optimization (say, minimization) problem, a solution p is said to dominate another solution q if

$$\forall i,\ f_i(p) \leq f_i(q), \text{ and } \exists j, \text{ such that } f_j(p) < f_j(q) \tag{45}$$

where $f_i|_{i=1,\ldots,M}$ are the objective functions. The set of the optimal non-dominated solutions are called Pareto-optimal set.

IV. Multi-Objective Planning Algorithm for Reactive Power Compensation Using MOPSO

In this section, the planning algorithm is provided in detail along with the brief discussion on MOPSO.

A. PSO: A Brief Overview

PSO is a population-based multi-point search technique [23] that mimics the social behavior of a flock of birds and a fish school. The search starts with a population of search points called particles. Each particle is encoded by a position vector (X), containing multi-dimensional information (initially chosen at random), which is updated by using particle's velocity (initially chosen at random) in successive iterations. The velocity vector (PV) of a particle is updated using its own previous

best position ($pbest$) and the best neighborhood particle's position ($nbest$). The best neighbor for a particle is also called leader/guide particle. The particle velocity and position update equations for mth particle nth dimension are

$$PV_{mn}^{iter+1} = wPV_{mn}^{iter} + \varphi_1 rn_1(pbest_{mn}^{iter} - X_{mn}^{iter}) + \varphi_2 rn_2(nbest_{mn}^{iter} - X_{mn}^{iter}) \quad (46)$$

$$X_{mn}^{iter+1} = X_{mn}^{iter} + PV_{mn}^{iter+1}. \quad (47)$$

Among the three component terms in (46), the first term is referred to as *momentum* or habit, i.e., the tendency of a particle to continue in the same direction it has been traveling. It is controlled by a variable inertia weight (w). The second and third terms, which are scaled by two learning constants (φ_1, φ_2) and two random numbers (rn_1, rn_2), are referred to as guidance by *self knowledge* and *collective knowledge*, respectively [24]. The position of a particle is updated with its current velocity using (47). The fitness of a particle is determined by a pre-defined objective function.

B. MOPSO: A Brief Overview

MOPSO is a version of PSO to solve multi-objective optimization problems, in which a particle has multiple fitness values. There are many MOPSO variants and the state-of-the-art review can be obtained in [25]. Most of the approaches belong to the Pareto-dominance based approaches. The main goals of all these approaches are to obtain a set of non-dominated solutions closer to the set of the Pareto-optimal solutions (i.e., better convergence) and to get diversified solutions (i.e., better diversity among the solutions). Better convergence can be achieved by the selection of proper guide for each particle. Two MOPSO variants used in this work are NSMOPSO and SPEA2-MOPSO. NSMOPSO is inspired from the philosophy of non-dominated sorting genetic algorithm-II [26]. In NSMOPSO, the non-dominated solutions are determined from the population members of the current iteration and the previous iteration. Then, all non-dominated solutions are sorted according to niche mechanism [22]. A set of the guides is formed using a given number of better ranked solutions. In any iteration, a particle randomly selects its own guide from the set of the guides. In SPEA2-MOPSO, an elite archive is created to preserve the non-dominated solutions found by the optimization algorithm and then it is used to assign fitness to each member of the archive itself and the current population undergoing evolution. The fitness assignment scheme of SPEA2 [27] is used in assigning a single fitness value for a particle from multiple objectives according to its non-domination rank and solution density [22], [28]. The guide selection for a particle in SPEA2-MOPSO is done according to the global best ($gbest$) topology of PSO [24].

C. Planning Algorithm

The planning algorithm consists of two important support subroutines, i.e., particle encoding/decoding scheme and load flow with UPQC-PAC model. A particle in MOPSO consists of three segments with the direct information of: 1) UPQC location in the network, 2) the amount of reactive power compensation required, and 3) K_{Se}. During the decoding process, the first segment of a particle is always converted to its nearest integer number. The solutions violating the third constraint are penalized. The pseudocodes for the complete planning algorithm are shown in Fig. 3.

Begin
// η_{pop} = size of MOPSO population
// η_{gen} = Maximum number of iterations
Generate *initial population* for MOPSO randomly using the *encoding scheme* (both position and velocity);
Decode the *particles* and calculate the objective functions;
Find the *initial non-dominated solutions*;
Find out initial set of guides;
iteration=1;
While *iteration*<= η_{gen}
  For *i*=1,...,η_{pop}
    Assign a guide for particle *i* from the set of guides;
    Update *velocity* and *position* of the particle;
    Decode *particle* to get the location and parameters for UPQC;
    Perform load flow incorporating the UPQC-PAC model;
    Calculate the *objective functions*;
  Endfor
  Find out the *non-dominated solutions*;
  Find out the new set of guides;
  iteration=*iteration*+1;
Endwhile
The final set of non-dominated solutions consists of optimal location, size, and the parameters for UPQC;
End

Fig. 3. Pseudocodes for the reactive power compensation planning with UPQC allocation using MOPSO.

TABLE I
MOPSO PARAMETERS

MOPSO parameters	33-node system	69-node system
Population size	300 (400 in *Case C*)	500 (600 in *Case C*)
Maximum number of iterations	100 (200 in *Case C*)	200 (300 in *Case C*)
Learning constants	(2.5, 2)	(2.5, 2)
Inertia weight	(0.4, 0.1)	(0.4, 0.1)

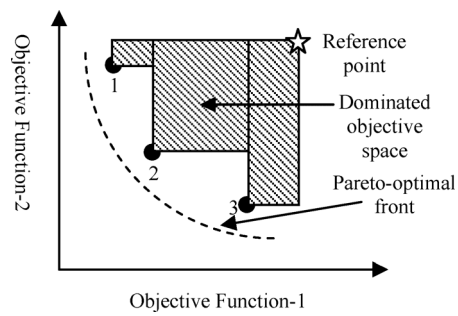

Fig. 4. Illustration of the dominated objective space.

V. SIMULATION RESULTS

A simulation study is performed to validate the proposed planning approach using two test distribution networks: 1) 33-node and 2) 69-node systems. The system data are available in [31] and [32], respectively. Both the systems have one substation located at node 1 and all other nodes are load nodes. The substation voltage is specified to be $1\angle 0$ p.u. The optimal reactive power compensation is determined considering the

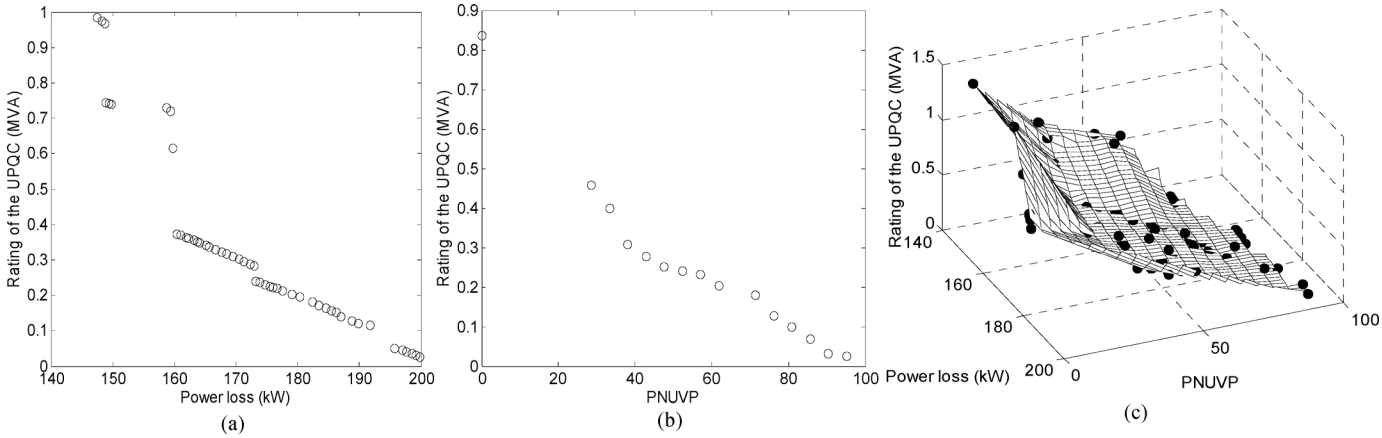

Fig. 5. PAFs obtained with the 33-node system for the planning: (a) *Case A*, (b) *Case B*, and (c) *Case C* (PAF along with Pareto-approximation surface).

peak load demand at each node. Firstly, a performance comparison between SPEA2-MOPSO and NSMOPSO is given. Then, the results of different planning cases are presented and analyzed. The results obtained with different load levels are provided. A comparative study with two-point reactive power compensation is shown. The THD of the load current is assumed to be 0.2 and the minimum voltage sag to be mitigated is assigned as 25% (i.e., $K_{Se} \geq 0.5$). The MOPSO parameters are optimized using repetitive runs and the optimized parameters are shown in Table I.

A. Performance Comparison Between NSMOPSO and SPEA2-MOPSO by Statistical Test

In multi-objective optimization, there exists a set of non-dominated solutions. A set of optimal non-dominated solutions constitutes a Pareto-optimal set. Since the meta-heuristic algorithms like PSO can not guarantee to provide the Pareto-optimal set, the set of non-dominated solutions obtained at a simulation run is called Pareto-approximation set [22]. The two-dimensional plot (for two-objective problems) of a Pareto-approximation set is known as Pareto-approximation front (PAF). For a problem with more than two objectives, the plot of a Pareto-approximation set is a Pareto-approximation surface. A typical PAF consisting of three non-dominated solutions is shown in Fig. 4 with dark circles. The quality of a PAF is assessed using the following indicators:

1) Hypervolume indicator: It is an indicator used to measure the portion of objective space dominated by the Pareto-approximation set with respect to a reference point [33] as indicated in Fig. 4. A higher hypervolume indicator signifies larger area dominated by the approximation set indicating that it is closer to the Pareto-optimal front (i.e., better convergence). In this work, firstly, the Pareto-approximation sets obtained with multiple simulation runs are normalized with respect to 1 MVA and 205 kW. Then, the hypervolume indicator is calculated considering the reference point as (1, 1).
2) Diversity indicator: The diversity indicator (Δ) for a problem with M objective functions, defined in (48), measures the diversity among the non-dominated solutions:

$$\Delta = \frac{\left(\sum_{j=1}^{N_{ndf}} |d_i - \overline{d}|\right)}{\left(N_{ndf}\overline{d}\right)} \tag{48}$$

where $d_i(\overline{d})$ is the distance (mean) between two neighboring solutions of a Pareto-approximation set and the number of solutions in the Pareto-approximation set is N_{ndf}. The diversity metric should ideally be zero. Thus, lower diversity indicator indicates better diversity among the solutions.

A statistical test is performed to compare the performances between SPEA2-MOPSO and NSMOPSO on the planning *Case A*. The results of 30 runs obtained with each algorithm are shown in Table II. The difference in view of the hypervolume indicator obtained with both the algorithms is very less ($< 1\%$). However, a better diversity is obtained with SPEA2-MOPSO. Hence, it is used in all subsequent studies. The PAFs obtained with the 33- and 69-node systems using SPEA2-MOPSO are shown in Figs. 5 and 6, respectively.

B. Results of Different Planning Cases

The PAFs obtained with the planning *Case A* are shown in Figs. 5(a) and 6(a) for both the networks. Each solution represents a different combination of the location and size for UPQC. The power losses of the uncompensated networks (i.e., without UPQC) are 202.67 kW and 224.98 kW for the 33- and 69-node networks, respectively. The result shows that significant amount of loss reduction can be obtained with UPQC allocation. The voltage at any node less than the allowable limit is said to have the undervoltage problem. With a limit of 0.95 p.u., 21 nodes of the 33-node (i.e., 63.63%) and 9 nodes of the 69-node (i.e., 13.04%) networks have the undervoltage problem without UPQC. The PAFs obtained with the planning *Case B* are shown in Figs. 5(b) and 6(b) for both the networks. The results illustrate that a UPQC rated around 0.8 MVA is sufficient to bring out all nodes from the undervoltage problem. On the contrary, the rating of UPQC as determined in [21] for

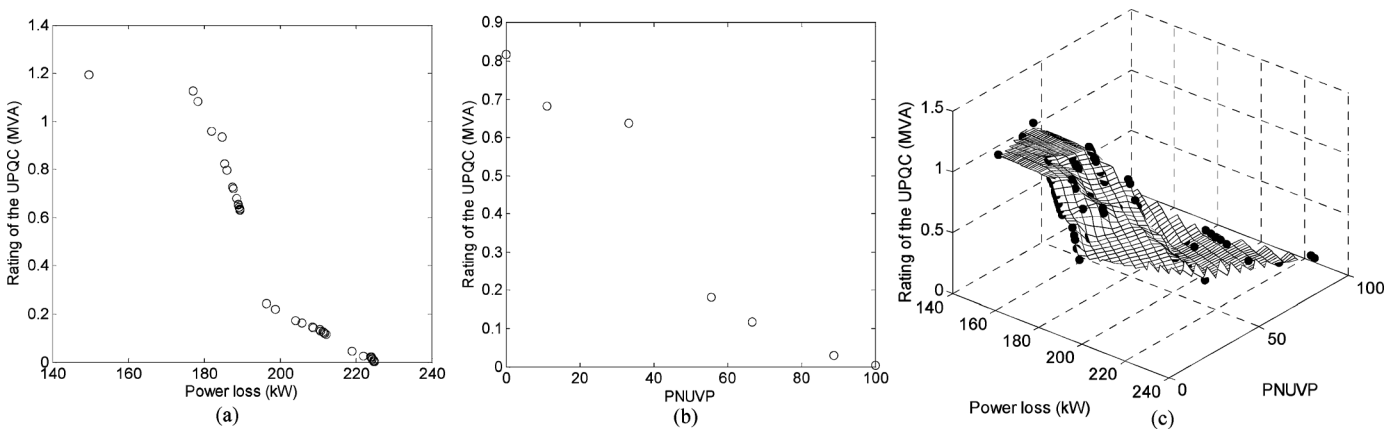

Fig. 6. PAFs obtained with the 69-node system for the planning: (a) *Case A*, (b) *Case B*, and (c) *Case C* (PAF along with Pareto-approximation surface).

TABLE II
PERFORMANCE COMPARISON BETWEEN SPEA2-MOPSO AND NSMOPSO WITH THE RESULTS OF 30 RUNS

Performance indicators	SPEA2-MOPSO		NS-MOPSO	
	Mean	Variance	Mean	Variance
Hypervolume	0.1907	1.095×10^{-6}	0.1924	7.534×10^{-7}
Diversity	1.2092	0.0064	1.4586	0.0034

TABLE III
SOLUTIONS WITH THE LOWEST POWER LOSS AND PNUVP

Sol.	Test network	UPQC location	K_{Se}	Q_{UPQC} (MVAr)	Rating of UPQC (MVA)	Power loss (kW)	PNUVP
(*Sol. A*)	33	7	1	0.8	0.9842	147.5	28.57
	69	61	0.5	1.11	1.194	149.7	33.33
(*Sol. B*)	33	6	0.5	0.81	0.8373	183.75	0
	69	57	0.6	0.78	0.8172	196.77	0

the same purpose is above 2 MVA for the 33-node network. Hence, the proposed approach provides more economical solution compared to [21]. In the 69-node system, the number of nodes with undervoltage problem without UPQC is 9. Thus, there exist only few solutions in the PAF. The PAFs obtained with the planning *Case C* are shown in Figs. 5(c) and 6(c) for both the networks. The Pareto-approximation surfaces on which the non-dominated solutions are located are drawn for better visualization.

It is noteworthy that UPQC with same rating located at different nodes in a network results in different power loss and PNUVP. Thus, there are multiple solutions with same UPQC rating in PAFs obtained with *Case C*. The solutions with the lowest power loss (*Solution A*) obtained with the planning *Cases A* and *C* and the solutions with the lowest PNUVP (*Solution B*) obtained with the planning *Cases B* and *C* are provided in Table III. The results illustrate that the MVA rating and the location for UPQC are different in both types of the planning. The power loss is significantly reduced due to the higher rated UPQC allocation. PNUVP is found to be non-zero in case of *Solution A*. This shows that the solutions corresponding to the lowest power loss fail to mitigate the undervoltage problem completely. Thus, PNUVP is chosen as one of the objectives for this planning problem.

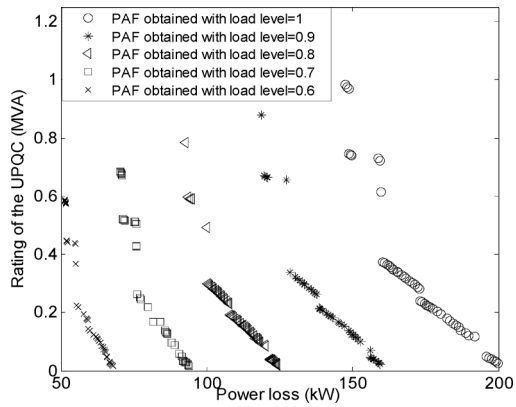

Fig. 7. PAFs obtained with different load levels for the 33-node system.

C. Results Obtained With Different Load Levels

In this work, the peak load demand of each node of a network is used in the determination of the optimal reactive power compensation. The reason is that a UPQC designed to operate at peak load demand can be operated in any other loading condition. Thus, a study on the UPQC-PAC allocation under different loading levels is carried out. The load demand at each node is computed by multiplying their respective peak demand with a load level. The PAFs obtained with the 33-node system are shown in Fig. 7. The result illustrates that the PAFs are of same pattern. However, the network power loss and the MVA rating for UPQC are obviously lower for the solutions obtained with lower load level because of the lesser load current at each line at lower load level. The optimal location for UPQC corresponding to a particular type of solution, for example the solution with the lowest power loss, in PAFs is found to be same, i.e., at node 7.

D. Comparison Between Single Point and Two-Point Reactive Power Compensation

The work is focused on single point reactive power compensation by allocating one UPQC in a network. Thus, it is interesting to have a performance comparison with two-point reactive power compensation, in which the optimal ratings and locations of two UPQCs are determined. This can be done by

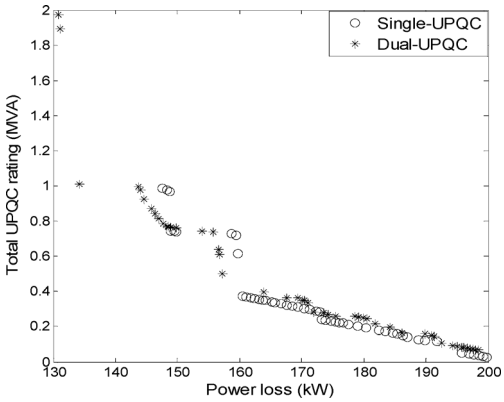

Fig. 8. PAFs obtained with single point and two-point reactive power compensations for the 33-node system.

TABLE IV
COMPARATIVE RESULTS OF REACTIVE POWER COMPENSATION WITH UPQC AND DSTATCOM [6]

Operational aspects	UPQC allocation		DSTATCOM allocation	
	Solution A	*Solution B*	*Solution A*	*Solution B*
UPQC location	61	57	61	61
Power loss (kW)	149.7	196.77	158.61	221.04
Minimum node voltage (p.u.)	0.9401	0.9587	0.9245	0.9492
MVA rating	1.19	0.82	0.924	2.68

changing the particle encoding of the SPEA2-MOPSO-based planning algorithm. A particle is encoded with the optimizing variables for two UPQCs. This increases the dimension for a particle from 3 (in case of single-point compensation) to 6. The comparative results of the 33-node system are shown in Fig. 8. It is observed that the single-point compensation is better option if the rating of UPQC is below 0.35 MVA because almost similar power loss is obtained with lower rated UPQC. If the rating of UPQC is more than 0.35 MVA the two-point compensation is better option. It is also observed that the solution corresponding to the minimum power loss is obtained with two-point compensation. But, the sum of two UPQC ratings is more than double compared to the single point compensation. The control of multiple UPQCs is also complex.

E. Performance Comparison With Reactive Power Compensation Using DSTATCOM Allocation

A quantitative performance comparison between the reactive power compensation with UPQC and DSTATCOM [6] allocations on the 69-node network is shown in Table IV. Since both DSTATCOM and network reconfiguration are simultaneously used in [6], the performance of DSTATCOM alone in reactive power compensation is considered to have a fair comparison. The solutions with the lowest power loss (*Solution A*) and the highest node voltage (*Solution B*) obtained with UPQC allocation are compared with those obtained with DSTATCOM allocation. The results show that better solutions in view of power loss and node voltage magnitude can be obtained with UPQC allocation and the MVA rating of UPQC are also comparable with DSTATCOM.

VI. CONCLUSION

A multi-objective planning for the reactive power compensation of radial distribution networks with UPQC allocation has been reported. In the proposed planning approach, the optimal location, the optimal reactive power compensation required at the location, and the parameters of UPQC are determined. The UPQC-PAC model is suitably modified so as to provide the reactive power compensation of a distribution network. Both the inverters participate in the reactive power compensation. The THD of load current is additionally included in the model. The UPQC-PAC model is suitably incorporated into the load flow algorithm of distribution systems. The contributions of this work are summarized as follows:

- The work shows that a UPQC which is traditionally used in power quality improvement of a single load can efficiently be used in reactive power compensation of a distribution network as well.
- It is shown that if a UPQC is optimally allocated and operated at healthy operating condition it can significantly reduce the power loss and improve the node voltage of a distribution network.
- The multi-objective planning approach with UPQC allocation provides a number of non-dominated solutions which facilitates in decision making for a utility to choose a final solution according to its capital expenditure budget and acceptable power loss and voltage profile of a network.
- The quantitative performance comparison shows that better solutions are obtained with the proposed approach compared to [6]. The approach also provides economical solutions compared to [21].
- The multi-point reactive power compensation provides better solution for higher rated UPQCs.
- The optimal locations for UPQC remain unchanged if the optimization is carried out with different load levels.

The allocation of multiple UPQCs can easily be done by changing the particle encoding of the algorithm. Some more features of UPQC can be incorporated into the planning model, for example voltage stability limit, line loadability, and load balancing. This needs future investigations.

REFERENCES

[1] D. Das, "Reactive power compensation for radial distribution networks using genetic algorithm," *Int. J. Elect. Power Energy Syst.*, vol. 24, pp. 573–581, 2002.
[2] M. Chis, M. Salama, and S. Jayaram, "Capacitor placement in distribution systems using heuristic search strategies," *Proc. Inst. Elect. Eng., Gener., Transm., Distrib.*, vol. 144, no. 3, pp. 225–230, 1997.
[3] R. Liang and Y. Wang, "Fuzzy-based reactive power and voltage control in a distribution system," *IEEE Trans. Power Del.*, vol. 18, no. 2, pp. 610–618, Apr. 2003.
[4] S. Deshmukh, B. Natarajan, and A. Pahwa, "Voltage/VAR control in distribution networks via reactive power injection through distributed generators," *IEEE Trans. Smart Grid*, vol. 3, pp. 1226–1234, 2012.
[5] M. Dadkhah and B. Venkatesh, "Cumulant based stochastic reactive power planning method for distribution systems with wind generators," *IEEE Trans. Power Syst.*, vol. 27, no. 4, pp. 2351–2359, Nov. 2012.
[6] S. Jazebi, S. H. Hosseinian, and B. Vahidi, "DSTATCOM allocation in distribution networks considering reconfiguration using differential evolution algorithm," *Energy Convers. Manage.*, vol. 52, pp. 2777–2783, 2011.
[7] V. Khadkikar, "Enhancing electric power quality using UPQC: A comprehensive overview," *IEEE Trans. Power Electron.*, vol. 27, no. 5, pp. 2284–2297, 2012.

[8] H. Fujita and H. Akagi, "The unified power quality conditioner: The integration of series- and shunt-active filters," *IEEE Trans. Power Electron.*, vol. 13, no. 2, pp. 315–322, 1998.
[9] M. Basu, S. P. Das, and G. K. Dubey, "Comparative evaluation of two models of UPQC for suitable interface to enhance power quality," *Elect. Power Syst. Res.*, vol. 77, pp. 821–830, 2007.
[10] V. Khadkikar and A. Chandra, "UPQC-S: A novel concept of simultaneous voltage sag/swell and load reactive power compensations utilizing series inverter of UPQC," *IEEE Trans. Power Electron.*, vol. 26, no. 9, pp. 2414–2425, 2011.
[11] D. O. Kisck, V. Navrapescu, and M. Kisck, "Single-phase unified power quality conditioner with optimum voltage angle injection for minimum VA requirement," in *IEEE Proc. Power Electronics Specialists Conf.*, Bucharest, Romania, 2007, pp. 574–579.
[12] V. Khadkikar and A. Chandra, "A novel structure for three-phase four-wire distribution system utilizing unified power quality conditioner (UPQC)," *IEEE Trans. Ind. Applicat.*, vol. 45, no. 5, pp. 1897–1902, 2009.
[13] A. Jindal, A. Ghosh, and A. Joshi, "Interline unified power quality conditioner," *IEEE Trans. Power Del.*, vol. 22, no. 1, pp. 364–372, Jan. 2007.
[14] M. Brenna, R. Faranda, and E. Tironi, "A new proposal for power quality and custom power improvement: OPEN UPQC," *IEEE Trans. Power Del.*, vol. 24, no. 4, pp. 2107–2116, Oct. 2009.
[15] V. Khadkikar and A. Chandra, "A new control philosophy for a unified power quality conditioner (UPQC) to coordinate load-reactive power demand between shunt and series inverters," *IEEE Trans. Power Del.*, vol. 23, no. 4, pp. 2522–2534, Oct. 2008.
[16] A. Ghosh and G. Ledwich, "A unified power quality conditioner (UPQC) for simultaneous voltage and current compensation," *Elect. Power Syst. Res.*, vol. 59, pp. 55–63, 2001.
[17] S. B. Karanki, M. K. Mishra, and B. K. Kumar, "Particle swarm optimization-based feedback controller for unified power-quality conditioner," *IEEE Trans. Power Del.*, vol. 25, no. 4, pp. 2814–2824, Oct. 2010.
[18] H. Heydari and A. H. Moghadasi, "Optimization scheme in combinatorial UPQC and SFCL using normalized simulated annealing," *IEEE Trans. Power Del.*, vol. 26, no. 3, pp. 1489–1498, Jul. 2011.
[19] B. Han, B. Bae, H. Kim, and S. Baek, "Combined operation of unified power-quality conditioner with distributed generation," *IEEE Trans. Power Del.*, vol. 21, no. 1, pp. 330–338, Jan. 2006.
[20] N. G. Jayanti, M. Basu, M. F. Conlon, and K. Gaughan, "Rating requirements of the unified power quality conditioner to integrate the fixed speed induction generator-type wind generation to the grid," *IET Renew. Power Gener.*, vol. 3, no. 2, pp. 133–143, 2009.
[21] M. Hosseini, H. Shayanfar, and M. Fotuhi-Firuzabad, "Modeling of unified power quality conditioner (UPQC) in distribution systems load flow," *Energy Convers. Manage.*, vol. 50, pp. 1578–1585, 2009.
[22] K. Deb, *Multi-Objective Optimization using Evolutionary Algorithms*. New York, NY, USA: Wiley, 2004.
[23] Y. Shi and R. C. Eberhart, "A modified particle swarm optimizer," in *Proc. IEEE Congr. Evol. Computat.*, 1998, pp. 69–73.
[24] Y. Valle, G. K. Venayagamoorthy, S. Mohagheghi, J. Hernandez, and R. G. Harley, "Particle swarm optimization: Basic concepts, variants and applications in power systems," *IEEE Trans. Evol. Computat.*, vol. 12, no. 2, pp. 171–195, 2008.
[25] M. R. Sierra and C. A. Coello Coello, "Multi-objective particle swarm optimizers: A survey of the state-of-the-art," *Int. J. Computat. Intell. Res.*, vol. 2, no. 3, pp. 287–308, 2006.
[26] X. Li, "A nondominated sorting particle swarm optimizer for multiobjective optimization," *Lecture Notes in Comput. Sci.*, vol. 2723, pp. 37–48, 2003.
[27] E. Zitzler, M. Laumanns, and L. Thiele, SPEA2: Improving the Strength Pareto Evolutionary Algorithm ETH, Zurich, Switzerland, 2001, Computer Engineering and Networks Laboratory Technical Report–103.
[28] S. Ganguly, N. C. Sahoo, and D. Das, "Mono- and multi-objective planning of electrical distribution networks using particle swarm optimization," *Appl. Soft Comput.*, vol. 11, no. 2, pp. 2391–2405, 2011.
[29] V. Khadkikar, A. Chandra, A. O. Barry, and T. D. Nguyen, "Analysis of power flow in UPQC during voltage sag and swell conditions for selection of device ratings," in *IEEE Proc. Can. Conf. Elect. and Comput. Eng.*, Ottawa, ON, Canada, 2006, pp. 867–872.
[30] S. Ghosh and D. Das, "Method for load-flow solution of radial distribution networks," *Proc. Inst. Elect. Eng., Gener., Transm., Distrib.*, vol. 146, no. 6, pp. 641–648, 1999.
[31] M. E. Baran and F. F. Wu, "Network reconfiguration in distribution systems for loss reduction and load balancing," *IEEE Trans. Power Del.*, vol. 4, no. 2, pp. 1401–1407, Apr. 1989.
[32] J. S. Savier and D. Das, "Impact of network reconfiguration on loss allocation of radial distribution systems," *IEEE Trans. Power Del.*, vol. 22, no. 4, pp. 2473–2480, Oct. 2007.
[33] J. D. Knowles, L. Thiele, and E. Zitzler, A Tutorial of the Performance Assessment of Stochastic Multiobjective Optimizers ETH, Zurich, Switzerland, 2006, Computer Engineering and Networks Laboratory Technical Report–214.

Sanjib Ganguly (M'12) was born in 1981 in India. He received the B.E. and M.E. degrees in electrical engineering from Bengal Engineering and Science University and Jadavpur University, respectively. He received the Ph.D. degree from IIT Kharagpur in 2011.

His research interest includes power system operation and planning, evolutionary algorithms, and DFACTS technologies.